Monthly Notices
of the
ROYAL ASTRONOMICAL SOCIETY

MNRAS **465,** 1218–1226 (2017)
Advance Access publication 2016 October 27

doi:10.1093/mnras/stw2776

Gamma-ray novae: rare or nearby?

Paul J. Morris,[1]★ Garret Cotter,[1] Anthony M. Brown[2] and Paula M. Chadwick[2]

[1] *Oxford Astrophysics. Denys Wilkinson Building, Keble Road, Oxford OX1 3RH, UK*
[2] *Department of Physics and Centre for Advanced Instrumentation, Durham University, Durham DH1 3LE, UK*

Accepted 2016 October 24. Received 2016 October 19

ABSTRACT

Classical novae were revealed as a surprise source of γ-rays in *Fermi* Large Area Telescope (LAT) observations. During the first 8 yr since the LAT was launched, 6 novae in total have been detected to $>5\sigma$ in γ-rays, in contrast to the 69 discovered optically in the same period. We attempt to resolve this discrepancy by assuming all novae are γ-ray emitters, and assigning peak 1 d fluxes based on a flat distribution of the known emitters to a simulated population. To determine optical parameters, the spatial distribution and magnitudes of bulge and disc novae in M31 are scaled to the Milky Way, which we approximate as a disc with a 20 kpc radius and elliptical bulge with semimajor axis 3 kpc and axis ratios 2:1 in the *xy* plane. We approximate Galactic reddening using a double exponential disc with vertical and radial scaleheights of $r_d = 5$ kpc and $z_d = 0.2$ kpc, and demonstrate that even such a rudimentary model can easily reproduce the observed fraction of γ-ray novae, implying that these apparently rare sources are in fact nearby and not intrinsically rare. We conclude that classical novae with $m_R \leq 12$ and within $\approx$8 kpc are likely to be discovered in γ-rays using the *Fermi* LAT.

Key words: novae, cataclysmic variables – dust, extinction – gamma-rays: diffuse background – gamma-rays: general.

1 INTRODUCTION

Cataclysmic variables (CVs) are semidetached binary systems consisting of a white dwarf accreting from a lower mass stellar companion which has overfilled its Roche Lobe. They are progenitors for nova events, the most luminous and therefore most easily detectable subclass of which are the classical novae (CNe, CN singular). Such events are characterized by a typical increase in optical luminosity of a factor of 10^6 (Carroll & Ostlie 2006), powered by a thermonuclear runaway (TNR) on the surface of the white dwarf (e.g. Shara 1989). Though γ-rays were hypothesized to arise from the beta decay of proton-rich elements produced in the TNR by Clayton & Hoyle (1974), these were predicted to be in the $\sim$ 1 MeV range; hence, it came as something of a surprise when on 2010 March 10, the CV V407 Cyg was detected in γ-rays using the *Fermi* Large Area Telescope (LAT) during a CN outburst (Abdo et al. 2010). Due to the unusual nature of the Mira variable containing V407 Cyg, Abdo et al. (2010) hypothesized that the γ-ray emission arose as a consequence of the strong stellar wind absent from more typical CN systems, and concluded that γ-ray CNe would be exceptionally rare. Just over 2 yr later, V1324 Sco became the second CN observed in γ-rays (Cheung, Glanzman & Hill 2012a), which has now been joined by V959 Mon (Cheung et al. 2012b), V339 Del (Hays, Cheung & Ciprini 2013), V1369 Cen (Cheung, Jean & Shore 2013) and V5668 Sgr (Cheung et al. 2015) in being observed to more than 5σ certainty [See Ackermann et al. (2014) and Cheung et al. (2016) for a complete summary]. The γ-ray novae all exhibit very similar light curves, with some properties given in Table 1.

In contrast, in the first 8 yr since the LAT first began taking data in 2008 August, a total of 69 (Mukai 2016)[1] novae have been discovered optically. Many reasons have been put forward to explain this discrepancy, with one possibility being that we are only able to detect γ-rays from novae occurring close to the solar neighbourhood. Although a few CNe have robust distance measurements, distance estimates to all the identified detected γ-ray novae place them within 4.5 kpc, which supports the notion that they are all relatively nearby within the Milky Way (Ackermann et al. 2014; Cheung et al. 2016). The same authors note that with the exception of V407 Cyg, there is nothing to indicate any of the γ-ray novae are particularly unusual. Another possibility is that we can only observe the most luminous γ-ray novae. Additionally, as is likely the case in V407 Cyg (Abdo et al. 2010), such phenomena may be driven by unusual conditions in the local environment which can accelerate particles to the high energies required to produce >100 MeV photons.

In this paper, we investigate the apparent rarity of γ-ray novae by simulating a Galactic nova population using novae in M31 to determine their optical properties and the Galactic γ-ray novae for their corresponding high-energy ones.

★ E-mail: paul.morris@physics.ox.ac.uk

[1] Accessible at http://asd.gsfc.nasa.gov/Koji.Mukai/novae/novae.html

Table 1. Table listing key properties of the γ-ray detected novae based on the daily bin with the maximum *TS* value. See Ackermann et al. (2014), Cheung et al. (2016) and the contained references for more information on daily binned light curves and the V1369 Cen distance. The adopted distances to V407 Cyg and V1324 Sco are inferred from estimating the line-of-sight extinction relative to a RC star (Özdönmez et al. 2016) and V959 Mon from expansion parallax (Linford et al. 2015). Chochol et al. (2014) inferred the V339 Del distance from the maximum-magnitude rate of decline relation [e.g. Cohen (1985)] and Banerjee et al. (2016) use infrared emission from the nova shell of V5668 Sgr to infer its distance. V1369 Cen currently has no more reliable distance estimate. $F_{\rm GalDiff}$ is the flux attributed to the Galactic diffuse on the sky pixel spatially coincident with the position of each nova. The *TS* values correspond to the peak daily flux.

Nova	V407 Cyg	V1324 Sco	V959 Mon	V339 Del	V1369 Cen	V5668 Sgr
Peak daily flux, F_γ (10^{-7} ph s^{-1} m^{-2})	13.9±2.6	12.3±2.9	13.8±3.7	5.9±1.1	5.1±1.3	1.8±0.8
$F_\gamma/F_{\rm GalDiff}$	0.254	0.185	0.305	0.381	0.0897	0.0704
TS value	56.8	35.0	27.7	65.7	37.6	11.6
Distance (kpc)	3.5±0.3	4.3±0.9	1.4±0.4	3.2±0.3	2.5	1.5±0.2

2 THE γ-RAY NOVAE

2.1 V407 Cyg

First observed in 1936 during an outburst (Hoffmeister 1949), V407 Cyg is a relatively well-studied system. It belongs to a rare subgroup of CVs known as symbiotic Miras, in which the secondary is a pulsating red giant (RG) known as a Mira variable. The WD accretes from the RG wind rather than via an accretion disc. This distinction was made for the first time in 1994 by Kolotilov et al. (1998), whilst Meinunger (1966) deduced the period of the Mira pulsations to be 745^d, the phase of which determines the optical magnitude of the system, which typically resides between $m_V = 13.5$ and 17. Miras are believed to be surrounded by a dust envelope, a fact used by Munari, Margoni & Stagni (1990) to attribute a sine wave superimposed on the *B*-band peaks to the orbital period of the system. They speculate that ionizing radiation from the WD inhibits the dust formation except in a shadow cone-shaped region produced by the RG which causes a wavelength-dependent shift to be observed at various orbital phases. Munari et al. (1990) concluded that the orbital period was $P = 43 \pm 5$yr. A second nova-like flare occurred in 1998 (Kolotilov et al. 2003) lasting until 2002, with a peak magnitude of around 11 attained. It is unknown whether any γ-rays would have been produced.

V407 Cyg underwent its most recent nova outburst on 2010 March 10, the optical magnitude of which reached $m_V \approx 8$ at its peak. It was during this event that γ-rays were observed (Abdo et al. 2010), implying the two were related. Abdo et al. (2010) found that a γ-ray transient detection using the LAT was consistent with the established optical location of V407 Cyg with only a $0.^\circ040$ offset, giving a 95 per cent chance that the γ-rays had indeed originated from it, and crucially that no other high-energy sources were in the error circle. As V407 Cyg is an exceptional symbiotic system for which the proposed γ-ray emission mechanisms appeared related to its unusual nature, Abdo et al. (2010) concluded that the emission of γ-rays from CVs would be extremely rare.

2.2 V1324 Sco

V1324 Sco was discovered on 2012 May 22 with an *I*-band magnitude of $m_I = 19.5$ (Wagner et al. 2012), brightening to $m_I = 11$ by June 2. The optical peak of $m_V \approx 10$ occurred on June 20, and slowly declined, with the time to decline by two visual magnitudes $t_2 \approx 25$ d (Cheung et al. 2014). From spectroscopic evidence, V1324 Sco is reminiscent of an Fe II classical nova [compared to V407 Cyg, an He/N nova (Cheung et al. 2014)]. Such systems have strong Fe II lines present in their spectra thought to originate from interactions of the nova shell with a gas envelope from the secondary companion. Their presence is tied to the evolution of the secondary star (Williams 2012).

The discovery of a *Fermi* LAT-detected transient at a location consistent with the optical location of V1324 Sco confirmed it as the first CN source of >100 MeV γ-rays. This came as something of a surprise as the possible γ-ray emission mechanisms all appeared to be linked to the dense RG wind, not thought to be present in classical novae.

2.3 V959 Mon

V959 Mon was first identified as a γ-ray transient on 2012 June 22, making it the first nova for which the γ-ray discovery preceded the optical (Cheung et al. 2012b). This was largely as a result of its apparent close proximity to the Sun ($\approx 20^\circ$) during the classical nova outburst, consequently the peak optical magnitude and t_2 are unknown, and optical confirmation of the nova was only obtained in 2012 August (Fujikawa, Yamaoka & Nakano 2012) when $m_V = 9.4$.

Shore et al. (2013) concluded V959 Mon was an oxygen–neon nova by looking at the available spectroscopic data from around 55 d after the outburst. The overabundance of oxygen, neon and magnesium present in their ejecta are thought to originate from pre-outburst enrichment of the envelope of a white dwarf of mass close to the Chandrasekhar limit. Periodic oscillations observed in multiple wavelengths have been confirmed as orbital (Osborne, Beardmore & Page 2013), making V959 Mon the only γ-ray nova with orbital inclination along the line of sight ($P_{\rm ORB} = 0.2957 \pm 0.0007^d \approx 7.10 \pm 0.02$ h).

2.4 V339 Del

Discovered on 2013 August 14 by Yamaoka & Itagaki (2009) at an optical magnitude of 6.8, V339 Del reached a maximum brightness of $m_V = 4.43$ around 2 d later (Munari et al. 2013) and was visible to the naked eye. A measurement at $m_V \approx 17.1$ on 2013 August 13 implies a very fast rise to maximum, and Chochol et al. (2014) measured a fast decline, with the time to decline by two visual magnitudes $t_2 \approx 10$ d.

2.5 V1369 Cen

V1369 Cen was discovered by Seach et al. (2013) on 2013 December 2 but reached a first optical maximum of $m_V = 3.6$ (AAVSO[2])

[2] American Association of Variable Star Observers (http://aavso.org/lcg).

3 d later. The onset of γ-ray emission coincided with a second optical maximum Cheung et al. (2013), and Izzo et al. (2013) inferred that the nova is relatively nearby by considering equivalent widths of of the Na I doublet to estimate the extinction. Shore et al. (2014) also use spectra to estimate a distance of $\approx$2.4 kpc.

2.6 V5668 Sgr

The most recent confirmed γ-ray novae was discovered on 2015 March 15 by Seach (2015). Much like V1369 Cen, the visual AAVSO light curve exhibits multiple optical peaks with the first maximum at $m_V = 4.1$ (Cheung et al. 2016). Banerjee et al. (2016) infer a distance of $d = 1.54$ kpc from measuring the expansion parallax of the nova shell and argue that the multiple optical peaks are a manifestation of strong dust production causing optical emission to be re-radiated in the infrared and the exact geometry of the nova shell allowing some optical light to escape.

3 GALACTIC NOVA RATE

In order to simulate novae in the Milky Way, it is necessary to estimate their occurrence rate. The location of the Solar system within the Galactic disc complicates matters, as optical emission is scattered from dust grains in the interstellar medium (ISM). This causes interstellar extinction, making it impossible to view every nova in the Milky Way typically reducing us to $\approx$10 nova detections annually. In the past, estimates have ranged enormously from 11 to 260 yr^{-1} (Shafter 1997 and the references therein), demonstrating that deducing such a rate is non-trivial.

When attempting to deduce a nova rate, one of two approaches is typically taken. The first concerns Galactic data, in which distances are deduced to nearby novae and combined with assumptions regarding their spatial distribution, which manifest themselves as high uncertainties. Unless a CN occurs close enough that the nova shell can be spatially resolved allowing a distance to be inferred (e.g. Ribeiro et al. 2013), novae distances are notoriously difficult to measure and often involve the assumption that novae are standardizable candles (Cohen 1985). Deductions typically agree with the values of 29 ± 17 yr^{-1} derived by Ciardullo et al. (1990) or the 35 ± 11 yr^{-1} deduced by Shafter (1997). Conversely, Liller & Mayer (1987) estimated a rate of 73 ± 24 yr^{-1}, demonstrating the uncertainties present in this method.

An alternative approach is to consider extragalactic nova populations, and scale them to the Milky Way by using, for example, the mass to light ratio. An example of this is della Valle & Livio (1994), who infer a nova rate of 20 yr^{-1}, consistent with the lower end of the Galactic procedure. An advantage of this method is that a much larger sample of the nova population can be observed in a nearby galaxy, such as M31. Novae here are also approximately equidistant and can be assumed to have similar reddening along the line of sight.

For this work, we leave our Milky Way nova rate as a free parameter consistent with $\dot{N}_{\rm novae} = 35 \pm 11$ yr^{-1} to test whether a compatible rate is capable of reproducing the observed nova rate.

4 CNE POPULATION IN M31

Due to the advantages outlined above, it was decided to use information from an extragalactic nova population to determine the spatial distribution and optical luminosities of our simulated novae, with M31 being the obvious candidate on which to model our nova population due to its close proximity. A list of all observed novae in M31 dating back to 1909 is available [Max-Planck-Institut für extraterrestrische Physik (2015),[3] Pietsch et al. (2007) and Pietsch (2010) and the references therein]. To account for the relative orientation of Andromeda with respect to the line of sight, spatial binning was done elliptically, and defined differently for the disc and bulge regions.

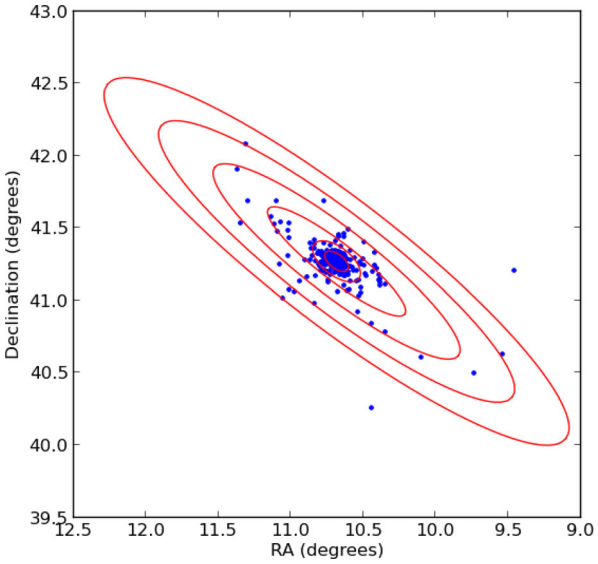

Figure 1. Figure demonstrating the spatial elliptical bins used for the novae in M31. Novae are shown as blue points, with the red ellipses showing the spatial bin boundaries. The inner two bins define the bulge, and have a different a/b compared to the outer four disc bins. Any novae outside of the largest ellipse were considered external to M31 and subsequently excluded. The inclination angle of the M31 semimajor axis relative to a line of constant declination is taken to be 37.°7 (de Vaucouleurs 1958).

The bulge-disc boundary and ratio of semimajor to semiminor axes, a/b, were defined according to isophotes detailed in Beaton et al. (2007). Hence we adopt $a_{\rm boundary} = 700$ arcsec, corresponding to a physical distance of 3 kpc considering the M31 distance of 780 kpc (Gil de Paz et al. 2007). Due to large number of bulge novae in M31, the bulge region was further subdivided into two sections each with the same a/b, with the inner–outer bulge boundary corresponding to $a = 350$ arcsec. The number of novae in each bin are subject to uncertainties caused by projection effects. These effects are not constant for each bin, but increase with the size of the semimajor axis, a_i, and scaleheight of the bin. Novae within the M31 disc are likely to be close to the Galactic plane, hence the dominant disc uncertainty is a_i. Bulge novae are likely to exhibit a larger range of heights above the plane; however, the larger sample and apparent symmetry of M31 should mitigate this effect.

For the disc, the ratio $a_{\rm disc}/b_{\rm disc}$ was defined based on the inclination angle of $i = 12.°5$ (Simien et al. 1978) with the maximum semimajor axis of $a = 4.°0$ consistent with 2.°0 the observed angular extent of M31 (de Vaucouleurs 1958). The disc region was subsequently divided into four linearly spaced sections, with the semiminor axes determined as $b = a\cos i$. Four sections were chosen as they allowed a better spatial distribution to be determined whilst containing multiple novae per bin. Binning is shown in Fig. 1.

Data from multiple filters were available, but due to being recent (oldest data from 1990), having a large sample size (274) and being less affected by interstellar extinction, it was decided to focus on the

[3] Accessible at http://www.mpe.mpg.de/m31novae/opt/m31/index.php

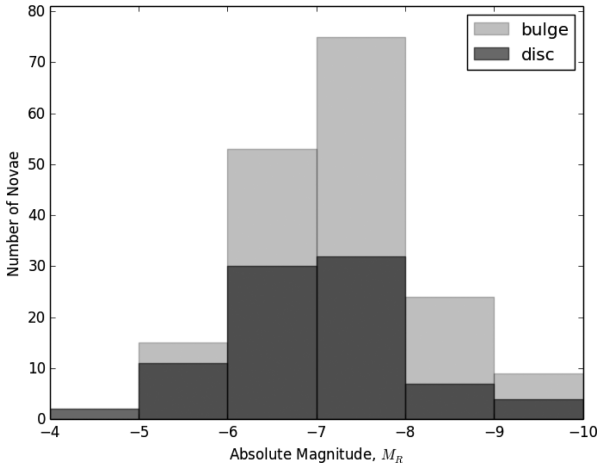

Figure 2. Histogram displaying the M_R values for the bulge and disc nova populations of M31. It can be seen that the two distributions are different, with a two-sample Kolmogorov–Smirnov test indicating a 26.5 per cent probability that the bulge and disc populations are intrinsically the same. Recurrent novae have been omitted from the original data of Max-Planck-Institut für extraterrestrische Physik (2015). With the exception of the $-5.0 < M_R \leq -4.0$ disc bin, each bin contains ≥4 novae.

R-band data. This list also includes recurrent novae (RNe), which are defined as those which have been observed multiple times with periods of quiescence which can last years to decades. RNe which have only been observed in outburst once are difficult to distinguish from CNe, although RNe are typically 1000 times less luminous (Carroll & Ostlie 2006). As γ-rays have not been detected from any typical RNe to $>5\sigma$, they should be emitted from any sample, and this was achieved by removing any novae with coordinates spatially consistent with other nova events. In total, 12 RNe were omitted, leaving 262 (176+86 = bulge + disc) novae. This is consistent with the result obtained by Shafter et al. (2015) who estimate ≈4 per cent of nova events in M31 are RNe. Dereddening corrections were applied by using the NASA/IPAC Extragalactic Database[4] value of $A_B = 0.300$ mag which is based on H I column densities (Burstein & Heiles 1982), with $A_R = (2.32/4.10)A_B$ using the mean extinction curves in (Savage & Mathis 1979). The absolute magnitude, M_R, of each nova could then be found, taking the distance to M31 to be 780 kpc.

Magnitude bin widths were chosen such that no bin was completely depleted of novae. It was decided that each bin should contain ≥4 novae, with 1 mag bin widths allowing for five bins under this criteria. The results are shown in Fig. 2. The likelihood of M31 bulge and disc novae being subsamples of the same population was assessed using a two-sample Kolmogorov–Smirnov (KS) test, and we cannot reject the null hypothesis that the populations are same to lower than 26.5 per cent. Even so, the assignment of absolute magnitudes to simulated novae was done separately for disc and bulge novae, and were based on the distribution of M_R values in Fig. 2. The counts per elliptical bin in Fig. 1 and histogram in Fig. 2 were converted to probability distributions, such that they could be used to assign radial and M_R values to a simulated nova population.

[4] https://ned.ipac.caltech.edu

5 PRODUCING CNE IN THE MILKY WAY

5.1 Milky Way distribution

For simplicity, we assume novae are found either in the bulge or disc, and neglect additional Galactic components. We define a Milky Way bulge semimajor axis of $a_b = 3.0$ kpc and disc radius of $R_d = 20$ kpc, and approximate the bulge in the xy plane as an ellipse with axis ratios 2:1 and set the angle $\phi = 20^\circ$ between the bulge semimajor axis and the vector between the Galactic Centre and Solar system (Binney, Gerhard & Spergel 1997). The M31 binned data were used to populate the Galactic plane with novae, with two concentric ellipses (a: $b = 1$: 0.5) describing the bulge region and four circles to mirror the number of M31 bins. The semimajor axes of these bins were obtained by normalizing the areas relative to M31, such that the equivalent Milky Way disc bin contains the same fraction of the M31 disc. Finally, to account for the larger size of M31, the number of novae in each M31 bin were divided by the apparent bin area and scaled accordingly to the Milky Way. The resulting novae counts were normalized, allowing each Milky Way bin to be populated with x and y positions assigned randomly but uniformly within the given bin (a_b was aligned along the x-axis). For disc novae, the z position was assumed to take the form $P(z) \propto \exp(-z/z_d)$, where z_d is the disc scaleheight. We adopt $z_d = 350$ pc (Dawson & Johnson 1994) to mirror the old disc population from which novae derive.

To deduce z positions for bulge novae, we tested several models from the literature. One was the bulge model of Binney et al. (1997) for the L-band surface brightness which we assume scales with stellar density, ρ_B, such that,

$$\rho_B = \rho_0 \frac{\mathrm{e}^{-a^2/a_m^2}}{(1 + a/a_0)^{1.8}}, \tag{1a}$$

$$a = \left(x^2 + \frac{y^2}{y_0^2} + \frac{z^2}{z_0^2} \right)^{1/2}, \tag{1b}$$

where ρ_0, a_m, a_0, y_0 and z_0 were all left as free parameters. Dwek et al. (1995) test different models for fitting the infrared surface brightness of the Galactic bulge, assessing each one with a χ_ν^2 fit. We test the application of some of their models to Galactic novae, namely,

$$\rho_1 = \rho_0 \exp(-0.5r^2), \tag{2a}$$

$$\rho_2 = \rho_0 r^{-1.8} \exp(-r^3), \tag{2b}$$

$$\rho_3 = \rho_0 \exp(-r), \tag{2c}$$

where r is defined by,

$$r = \left[\left(\frac{x}{x_0} \right)^2 + \left(\frac{y}{y_0} \right)^2 + \left(\frac{z}{z_0} \right)^2 \right]^{\frac{1}{2}}, \tag{3}$$

where the parameters ρ_0, x_0, y_0 and z_0 we left free. In order to evaluate these functions, a population of novae was simulated taking z values for the disc population as described previously, and using each function above to describe the bulge whilst varying the free parameters. This was done due to difficulties distinguishing between observed disc and bulge novae. Each fit was then compared to the observed sample via a two-sample KS test, with results displayed in Table 2.

Table 2. Table showing best-fitting parameters for the tested models with respect to reproducing the observed novae population. p_{KS} gives the probability that the simulated novae derive from the same global population as the observed novae. It can be seen that the best fit was obtained for the Gaussian model. Simulated populations were corrected for reddening effects using equation (5).

Model	ρ_0	x_0	y_0	z_0	a_0	a_m	p_{KS}
Equation (1a)	890	–	0.674	1.00	0.01	1.0	0.771
Equation (2a)	1×10^6	4.17	0.674	0.344	–	–	0.949
Equation (2b)	1×10^6	0.817	0.838	0.45	–	–	0.893
Equation (2c)	1×10^7	1.11	0.744	1.00	–	–	0.575

5.2 Milky Way reddening

Effects due to interstellar absorption must be accounted for when considering the number of novae in our simulations that it would be possible to detect in the *R*-band. To do this, we apply the *R*-band corrected double exponential dust distribution model of Dawson & Johnson (1994), such that the *R*-band extinction, $\alpha(r, z)$, at any point within the Milky Way in units of Δm_R kpc^{-1} along the line of sight is given by

$$\alpha(r, z) = \frac{A_R}{A_V}\alpha_{GC}\exp\left(\frac{-r}{r_d}\right)\exp\left(\frac{-|z|}{z_d}\right), \quad (4)$$

where $\alpha_{GC} = 9.4\, m_V\,\mathrm{pc}^{-1}$ and $A_R/A_V = 2.32/3.1$ (Fitzpatrick 1999). We assume that the spatial distribution of dust has scale-height $z_d = 0.2$ kpc, and again use the argument of Dawson & Johnson (1994, hereafter DJ) that the disc surface density decreases with scale distance $r_d = 5$ kpc, and assume that the Galactic dust traces this. We use the method of the same authors to compute the reddening along the line of sight to each nova in increments Δs of no greater than 50 pc, such that the total magnitude gain due to reddening effects is given by

$$\Delta m_R = \sum_i \alpha_i \Delta s_i. \quad (5)$$

We consider a nova to be detected if it has an apparent *R*-band magnitude less than a threshold magnitude, $m_R < m_{\mathrm{th}}$.

Reddening values were compared to those recently estimated from the SDSS maps by Schlafly & Finkbeiner (2011). For $\Delta m_R < 5$ in the DJ model, we obtain an rms residual value of 2.30. For $\Delta m_R < 10$, this increases to 4.87.

5.3 γ-ray properties

It was assumed that all novae emit in γ-rays. For a nova to be defined as a γ-ray source, we require $TS > 25$ (equivalent to 5σ when modelled using a simple power-law model) over the emission period. In order to assign each nova with a γ-ray luminosity, the 1-d bin peak values for the existing *Fermi* LAT detected γ-ray novae were taken, and a flat distribution assumed between them. The simulated novae were each assigned a γ-ray luminosity based on this distribution. This was done as a nova is more likely to be detected in γ-rays when at its peak. Although V5568 Sgr lacks a daily flux with $TS > 25$, it was still detected overall to $>5\sigma$ and its peak flux was included as the possibility remains that most of the γ-ray novae are more luminous than average. This assignment required the use of nova distances, which as previously discussed can be unreliable, as such the allowed γ-ray luminosity range was defined by the dimmest nova, V5668 Sgr, and the brightest V1324 Sco. Table 1 shows that the percentage uncertainty on the distance to each of these novae is ≈20 per cent. As $L_\gamma \propto d^2$, and these manifest themselves as ≈40 per cent uncertainties in L_γ when combined with the F_γ uncertainties. As such, we extend our luminosity range to account for these uncertainties; therefore, our nova population will contain novae with intrinsic luminosities consistent with the range of those observed.

In addition, the source in question must be visible against the sky background, which is described by the *Fermi* LAT background models gll_iem_v06.fits (Galactic diffuse) and iso_P8R2_SOURCE_V6_v06.txt (isotropic diffuse).[5] To quantify this, the overall background flux from the Galactic diffuse, F_{GalDiff}, was taken for the pixel containing each detected γ-ray nova, and the ratios of peak daily flux (with $TS > 25$) to background flux, $F_\gamma/F_{\mathrm{GalDiff}}$ were calculated. The effects of the isotropic diffuse were deemed insignificant due to the proximity of the γ-ray novae to the Galactic plane, and so was neglected. They are listed in Table 1. An additional criteria for γ-ray detection was therefore that the ratio $F_\gamma/F_{\mathrm{GalDiff}}$ was greater than the mean $F_\gamma/F_{\mathrm{GalDiff}}$, namely $[F_\gamma/F_{\mathrm{GalDiff}}]_{\mathrm{mean}} = 0.214$ for each simulated nova event. We therefore expect to see ≈6 γ-ray detected novae for every 69 which are *R*-band visible, equivalent to ≈8.7 per cent, if their apparent rarity is caused by proximity effects.

6 RESULTS

Results are based on 100 simulations each of 8-yr novae populations. Error bars are taken as the standard deviations of the 100 results, and so are quoted to 1σ.

We find that our model is best able to reproduce the correct number of observed novae when the global nova rate is $\dot{N}_{\mathrm{novae}} \approx 20\,\mathrm{yr}^{-1}$. Fig. 3 demonstrates the success of our model to reproduce the observed distribution of novae, and show that interstellar extinction effects are greatest when observing through the Galactic plane towards the Galactic Centre, thus coinciding with the region of the highest γ-ray background. This implies that the population of novae in the Milky Way is bulge dominated, much like in M31. Fig. 4 shows that our simulated population produces a fraction of novae consistent with observations for any limiting *R*-band magnitude with $m_{\mathrm{th}} < 13$. As novae in our M31 sample were as dim as $m_R = 20.6$, this is strong evidence to say such a rudimentary model can reproduce the observed γ-ray nova fraction, validating our assumptions. The fact that the number of γ-ray novae is consistent with being constant across the range of m_{th} values implies that the γ-ray sky background flux is the dominant factor prohibiting the discovery of further γ-ray novae. It can also be seen that at low m_{th} a γ-ray nova is more likely to be observed lacking an optical counterpart. Typically, there was one per simulation, so the unidentified γ-ray sources in the *Fermi* 3FGL catalogue are unlikely to contain many novae.

The axial symmetry of our assumed nova distribution is shown in Fig. 5. It can be seen that, like the observed novae, the simulated

[5] *Fermi* background models can be downloaded from http://Fermi.gsfc.nasa.gov/ssc/data/access/lat/BackgroundModels.html

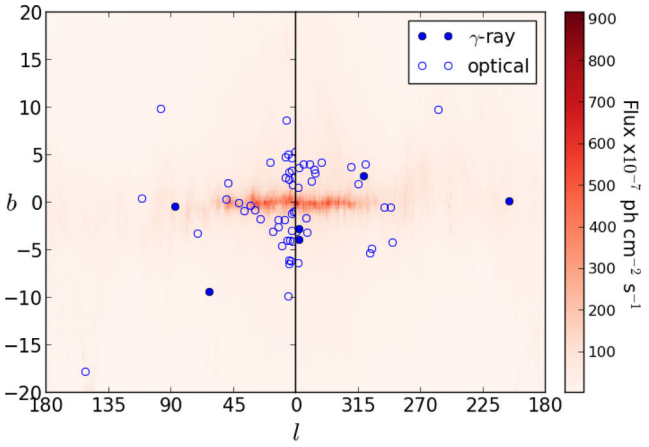

(a) Galactic Novae

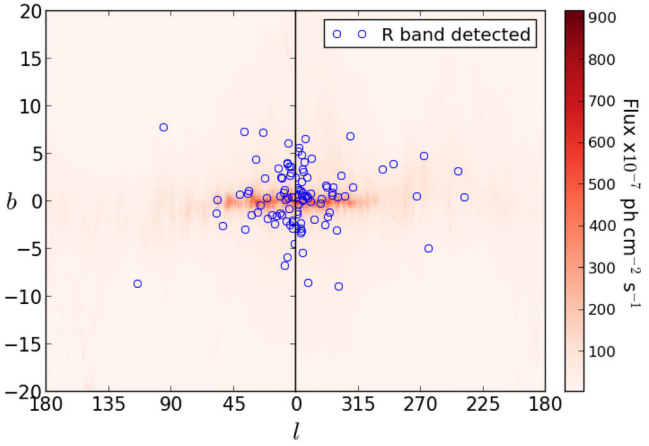

(b) Simulated Novae

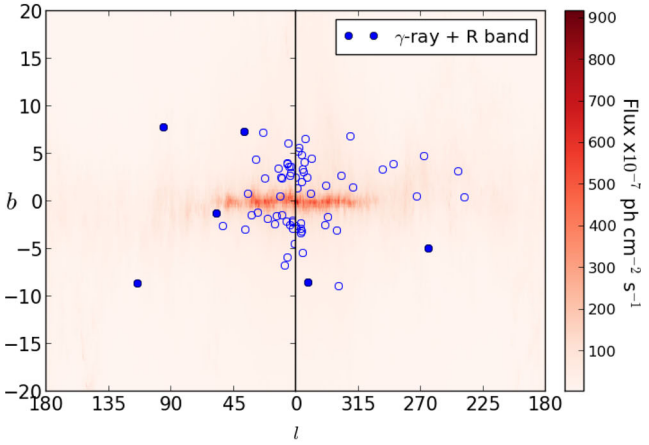

(c) Visible Novae

Figure 3. (a) Distribution of Galactic novae on the sky. (b) Example simulated population. (c) Visible novae accounting for interstellar extinction in our simulated population. The colour scale represents the intensity of the γ-ray sky background.

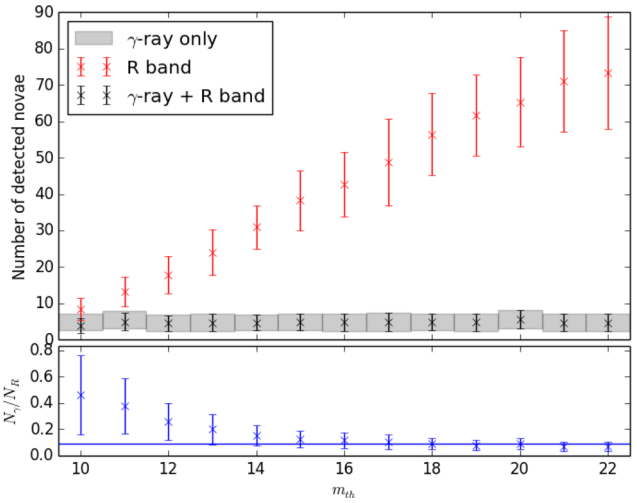

Figure 4. Figure showing how the number of R-band and γ-ray detected novae vary as a function of $m_{\rm th}$. It can be seen that for sufficiently dim $m_{\rm th}$, the predicted ratio is consistent with the observed ratio which is shown by the horizontal line in the lower panel. The error bars are taken as the standard deviation based on 100 runs of the code.

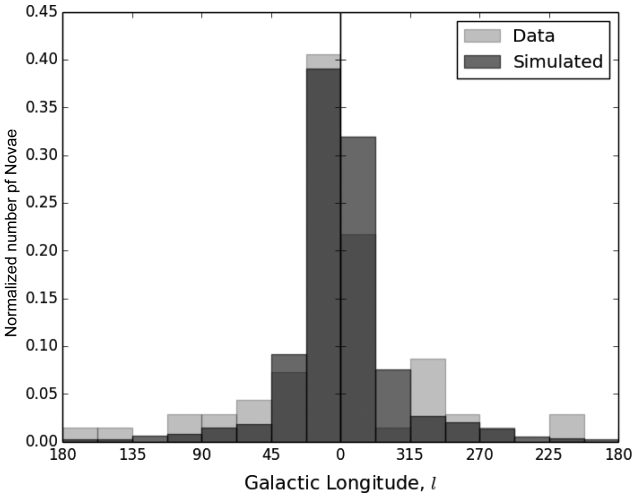

Figure 5. Comparison of the l values for Galactic novae to simulated novae, where the simulated novae have been assigned l values based on the spatial binning of M31 novae in Fig. 1 scaled to a Milky Way radius of 20 kpc. Although to a lesser extent than in the data, our model reproduces the asymmetry in the Galactic longitude distribution, which we attribute to the Solar system being closer to the bulge at $45 > l > 0$ relative to $360 > l > 315$.

novae have a larger population at $45 > l > 0$ relative to $360 > l > 315$, albeit to a lesser extent. We attribute this to the Solar system being closer to the Milky Way bulge at the smaller l values.

Fig. 6 illustrates the range of m_R values for the simulated novae as measured from Earth. It demonstrates that a large fraction of the total novae are far too dim to be observed realistically and that only CNe with $m_R \leq 12$ and within $\approx$8 kpc are likely to be discovered in γ-rays.

The assumed power-law distribution of novae γ-ray luminosities as a function of distance is displayed in Fig. 7. It can be seen that the effect of our assumed flat distribution is to broaden the effective index of the overall spectrum, and that all novae within $\approx$7 kpc with $F_\gamma > 5 \times 10^{-7}$ photons s^{-1} cm^{-2} are discovered both in γ-rays and the R-band, which is consistent with observations.

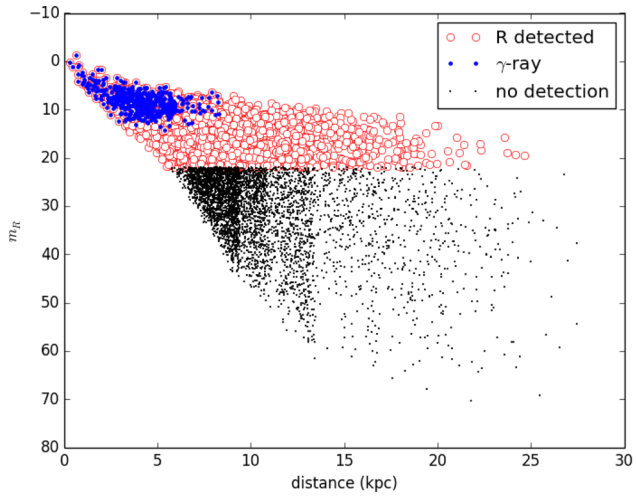

Figure 6. Figure demonstrating the detectability of novae with varying m_R as a function of distance. In this case, $m_{\rm th} = 22$.

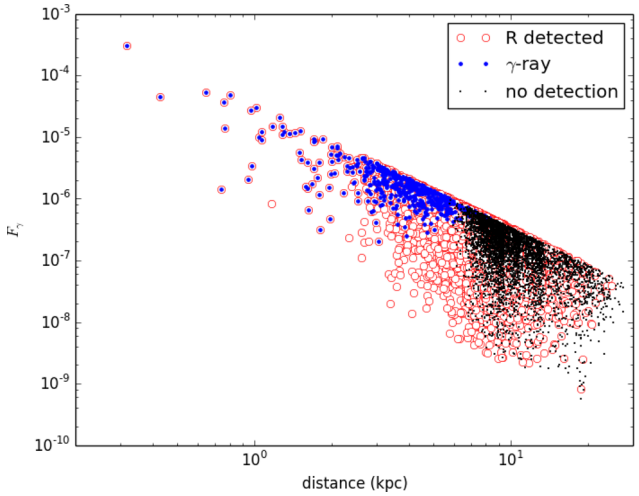

Figure 7. Figure demonstrating the detectability of novae with varying m_R as a function of distance. In this case, $m_{\rm th} = 22$. It can be seen that the assumed power-law relationship is recovered, and that the majority of novae detected within 5 kpc are detected both in γ-rays and in the R-band.

The figure indicates that we should be able to optically confirm the majority of novae within ≈7 kpc from us.

7 DISCUSSION

As this study has been based on observed novae in M31, any intrinsic differences between the M31 and MW novae must be discussed. It is clear from Fig. 2 that M31 has a bulge-dominated nova population, which is something we cannot directly confirm for the MW due to our location within the disc and the aforementioned difficulties in measuring novae distances, which impose restrictions on our ability to deduce this. It has been hypothesized that barred spiral galaxies can drive star formation in galactic centres, and Athanassoula & Beaton (2006) use near-infrared data for M31 to conclude that it is a barred spiral much like our Milky Way. The bar can transfer gas and drive star formation in the bulge, thus leading to a higher stellar population than in the disc, and therefore more binary systems, some of which will be CVs capable of producing nova outbursts. This can explain the observed bulge-dominated population, and the similarity of M31 to the MW suggests the MW nova population need also be bulge dominated and justifies our use of M31 novae. It is unlikely that the M31 nova population is an observational artefact caused by reddening effects exclusive to the disc, and we reproduce the distribution of MW novae on the sky implying a bulge-dominated population, contradicting the findings of Hatano et al. (1997) who find M31 has a disc-dominated nova population.

We find that adjusting the bulge-to-disc nova fraction has very little effect on overall nova rates in either waveband, but a larger effect on the sky distribution, whereby the simulated coordinates diverge from those observed. This is a consequence of the binning criteria as disc bins closer to the Galactic Centre contain more novae. Therefore the effect of reducing the proportion of bulge novae is effectively to shift them to the inner bin of the disc, where those on the near side to the Solar system are mostly observed and those further away are not. It is clear that the bin immediately surrounding the bulge contains the largest errors which are not taken into account, both from bulge related projection effects in obtaining the M31 distribution and defining a definite bulge boundary. Strong reddening and γ-ray background levels in these regions mitigate these effects to the extent that making the MW bulge semimajor axis 2 kpc has very little impact on the number of novae which can be detected.

Fig. 5 implies M31 and MW novae are distributed in a similar manner, and two-sample KS tests on the output simulated distribution give a ≈50 per cent chance that the distributions can arise from samples of the same global population. The discrepancies arise at points far from the Galactic Centre, in regions of low interstellar extinction, implying novae need be slightly more spread out in the Milky Way relative to Andromeda. This could be because our simulated Milky Way is smaller than M31 ($R_{M31} = 27$ kpc; de Vaucouleurs 1958), but a more likely explanation is that our nova sample is not large enough. For a complete sample, we would not expect to see empty l bins, though depleted bins could be indicative of areas with higher interstellar extinction. Due to difficulties in measuring reddening effects, we conclude that any lack of longitudinal symmetry exhibited by observed Galactic novae instead highlights the difficulties in modelling Galactic reddening, and that reddening effects need not be symmetric about the MW centre. Furthermore, novae can occur in any region on the sky, hence regions with preferential sky coverage are likely to contain more novae, imposing a bias on our data set.

Figs 6 and 7 show the range of values for m_R and F_γ when both are a function of distance. These essentially explain how γ-ray and R-band light propagate through our simulated Milky Way. The large spread for m_R is a direct manifestation of the range of interstellar extinction values experienced by novae with significantly different line-of-sight paths to the Solar system. In contrast, the spread in F_γ only reflects that of the defining population; hence, the index is reasonably approximated by a power law. This again highlights the importance of accurately determining interstellar extinction. Fig. 7 exhibits a sudden cutoff in detectability (blue to black transition) occurring between $d \approx 6$ and 7 kpc. This is because in our simulations the Solar system is located 8 kpc from the Galactic Centre and ≈6 kpc from the nearest point of the elliptical bulge, and novae in this region are both more likely to be dominated by the γ-ray sky background and experience stronger extinction effects, rendering them undetectable.

Despite the importance of interstellar extinction with respect to nova discovery, the γ-ray sky background completely dominates

when attempting to discover γ-ray novae. Fig. 3 demonstrates that novae observed in γ-rays are typically not close to the Galactic plane, something which our simulated population in Fig. 3 reproduces. This is a direct consequence of the γ-ray background being significantly smaller further from the Galactic plane. One particular consequence of this is that any optically unassociated object in the *Fermi* LAT catalogue (Acero et al. 2015) are unlikely to be classical novae. Novae observed at high $|l|$ are more likely to be nearby simply for geometrical reasons, less likely to suffer optically from interstellar extinction and more likely to be discovered in γ-rays due to the lower background. This combination of facts essentially explains the relative ease with which our rudimentary model can reproduce the fraction of γ-ray novae.

With regards to observing a CNe in both γ-rays and the *R*-band, Figs 6 and 7 are of particular interest. The blue region (dark grey in printed version) in Fig. 6 indicates that we can only realistically expect to detect novae in γ-rays for $m_R < 12$ and $d \leq 8$ kpc, with the majority of these within 6 kpc. These figures can be used to explain that the non-detection of Nova KT Eri [distance 6.3 ± 0.1 kpc (Raj, Banerjee & Ashok 2013), $m_V = 8.1$ (Yamaoka & Itagaki 2009)] is as a result of the nova being less luminous in γ-rays than those discovered. Raj et al. (2013) also discusses the possibility of KT Eri being a recurrent nova, and hence may not belong to the same class of objects. Again, these numbers are the manifestation of parameters in our model. Looking in the $l = 0$ direction, novae can only be detected optically and in γ-rays away from the Galactic plane. Whilst optical novae trace Galactic reddening, γ-ray fluxes follow an inverse square law and so only the more luminous novae can be observed further away than 6 kpc. Even then, they need to be located in a region of low enough γ-ray background, which is unlikely given the bulge-dominated spatial distribution. Neglecting off-plane effects, this represents $\approx (6\,\mathrm{kpc}/20\,\mathrm{kpc})^2 = 9$ per cent fraction of our Galaxy, which is close to the observed 8.7 per cent of CNe detected in γ-rays. This simple argument supports the fact that γ-ray novae are rare only because they need to be close by to be detected.

The number of identifiable γ-ray detectable novae is independent of $m_{R,\,\mathrm{th}}$, and Fig. 4 illustrates that the ratio N_γ/N_R decreases with increasing $m_{R,\,\mathrm{th}}$. Whilst N_γ/N_R can be tweaked by the number of *R*-band novae visible, N_γ is always consistent with observations, and depends only on the global nova rate, which is optimized at $\dot{N}_{\mathrm{novae}} \approx 20\,\mathrm{yr}^{-1}$. Although lower than the inferred rate of Shafter (1997), we deem our conclusions still valid as the goal was to reproduce the observed nova population on the sky, and from that draw conclusions about the number of γ-ray novae. The same argument applies to our redding parameters, where we use $z_d = 0.2$ kpc instead of the original $z_d = 0.1$ kpc used by DJ. This was necessary to avoid a large population of novae in the range $2 > |b| > 0$ which is not observed.

Referring to Table 1, it is clear that V1324 Sco, V1369 Cen and V5668 Sgr were detected with the LAT with ratios $F_\gamma/F_{\mathrm{GalDiff}} < [F_\gamma/F_{\mathrm{GalDiff}}]_{\mathrm{mean}} = 0.214$. Therefore it is possible that novae in our simulations, not considered detectable at γ-ray energies, would have indeed been detected by *Fermi*, therefore increasing our ratio N_γ/N_R. On average, this effect would cancel with those with $F_\gamma/F_{\mathrm{GalDiff}} > [F_\gamma/F_{\mathrm{GalDiff}}]_{\mathrm{mean}} = 0.214$ located in regions of the sky with high background fluxes. Such an event can be attributed to our simulated γ-ray luminosities being based off a sample of only six novae. V5668 Sgr is of particular interest because it implies that the nova was intrinsically fainter in γ-rays than the others. Transient phenomena are always subject to a bias favouring those events which are more luminous due to their ease of discovery and study. Thus, our simulated γ-ray population may be more luminous on average than the global population, assuming all novae do emit γ-rays. If this were the case, we would expect to see fewer γ-ray novae reducing our N_γ/N_R. Clearly, any future studies on γ-ray novae would benefit from a larger source sample size, which would give insight into the number of novae per unit energy and could replace the assumed flat distribution.

8 CONCLUSIONS

Assuming Milky Way novae are similar in the *R*-band magnitude and spatial distribution to M31, a population of novae was simulated over the first 8 yr of *Fermi* LAT observation time, during which 6 out of 69 have been detected in γ-rays. This was done by dividing M31 into two bulge and four disc spatial bins, and binning the *R*-band magnitudes of novae for both bulge and disc. Simulated novae were assigned the *R*-band peaks based on their spatial location (disc or bulge) in the Milky Way, with Milky Way spatial bins for the disc and bulge separately normalized such that they contain the same fractional areas as their M31 counterparts. M31 nova rates were computed per unit area on the sky, and scaled to the Milky Way, allowing a simulated Galactic nova population to be produced. We assumed a Galactic disc of radius $R_{\mathrm{MW}} = 20$ kpc and a bulge with semimajor axis $a = 3.0$ kpc with 2D axis ratios 2:1.

The spatial locations of simulated novae were converted to galactic coordinates. The longitude was done geometrically, whereas the latitude form disc novae assumed exponential decay profiles of scaleheights $z_d = 350$ pc, whilst bulge novae were found to best follow a Gaussian profile, $\rho_1 = \rho_0 \exp(-0.5r^2)$, with $r = [(x/x_0)^2 + (y/y_0)^2 + (z/z_0)^2]^{0.5}$ and best-fitting parameters $\rho_0 = 1 \times 10^6$, $x_0 = 4.17$, $y_0 = 0.674$ and $z_0 = 0.344$. Optically, the double exponential disc extinction model of DJ was assumed, allowing the total amount of reddening in the *R*-band along the line of sight to be determined. This yielded an m_R value for each nova, which if was smaller than the free parameter $m_{R,\,\mathrm{th}}$, led the nova to be classed as discoverable in the *R*-band.

Simulated novae were assigned γ-ray peaks based on a flat distribution of 24 h bin maximum *TS* values for the existing novae light curves and assuming an inverse square law relationship between γ-ray peak and distance, the γ-ray flux was calculated at the Earth. This was then compared to the average γ-ray background flux at the location on the *Fermi* LAT all sky map consistent with the location of each nova. If the nova flux was greater than the threshold of $[F_\gamma/F_{\mathrm{GalDiff}}]_{\mathrm{mean}} = 0.214$, it was recorded as a detection in γ-rays.

We find that for all values of m_{th}, the number of novae observable in γ-rays, N_γ, is consistent with the number both observable in γ-rays and the *R*-band, with only small exceptions present for small m_{th}. We attribute this to the γ-ray background being the most significant hindrance to the discovery of γ-ray novae. Our simulations tell us that any given nova is unlikely to be discovered in γ-rays if $m_R \geq 12$ and $d > 8$ kpc, and that the ratio N_γ/N_R is consistent with the observed ratio for all $m_{R,\,\mathrm{th}} < 13$. This demonstrates that observed nova rates can easily be reproduced with sensible parameters from a simple model, implying that γ-ray novae are indeed nearby rather than intrinsically rare phenomena.

ACKNOWLEDGEMENTS

This work was supported by the Oxford Centre for Astrophysical Surveys which is funded through generous support from the

Hintze Family Charitable Foundation. GC acknowledges support from STFC grants ST/N000919/1 and ST/M00757X/1 and from Exeter College, Oxford. We would also like to thank Retha Pretorius and Matt Ridley for useful discussions about novae and galactic dynamics, and the Department of Physics at Durham University.

REFERENCES

Abdo A. A. et al., 2010, Science, 329, 817
Acero F. et al., 2015, ApJS, 218, 23
Ackermann M. et al., 2014, Science, 345, 554
Athanassoula E., Beaton R. L., 2006, MNRAS, 370, 1499
Banerjee D. P. K., Srivastava M. K., Ashok N. M., Venkataraman V., 2016, MNRAS, 455, L109
Beaton R. L. et al., 2007, ApJ, 658, L91
Binney J., Gerhard O., Spergel D., 1997, MNRAS, 288, 365
Burstein D., Heiles C., 1982, AJ, 87, 1165
Carroll B. W., Ostlie D. A., 2006, An Introduction to Modern Astrophysics and Cosmology, 2nd edn. Pearson, San Francisco
Cheung C. C., Glanzman T., Hill A. B., 2012a, The Astron. Telegram, 4284
Cheung C. C., Shore S. N., De Gennaro Aquino I., Charbonnel S., Edlin J., Hays E., Corbet R. H. D., Wood D. L., 2012b, The Astron. Telegram, 4310
Cheung C. C., Jean P., Shore S. N., 2013, The Astron. Telegram, 5653
Cheung C. C., Shore S. N., Jean P., on behalf of the Fermi-LAT Collaboration, 2014, Am. Astron. Soc. Meeting Abstr., 223, 113
Cheung C. C., Jean P., Collaboration Fermi Large Area Telescope, Shore S. N., 2015, The Astron. Telegram, 7283
Cheung C. C. et al., 2016, ApJ, 826, 142
Chochol D., Shugarov S., Pribulla T., Volkov I., 2014, Contrib. Astron. Obs. Skalnate Pleso, 43, 330
Ciardullo R., Tamblyn P., Jacoby G. H., Ford H. C., Williams R. E., 1990, AJ, 99, 1079
Clayton D. D., Hoyle F., 1974, ApJ, 187, L101
Cohen J. G., 1985, ApJ, 292, 90
Dawson P. C., Johnson R. G., 1994, J. R. Astron. Soc. Can., 88, 369 (DJ)
de Vaucouleurs G., 1958, ApJ, 128, 465
della Valle M., Livio M., 1994, A&A, 286
Dwek E. et al., 1995, ApJ, 445, 716
Fitzpatrick E. L., 1999, PASP, 111, 63
Fujikawa S., Yamaoka H., Nakano S., 2012, Cent. Bur. Electron. Telegrams, 3202
Gil de Paz A. et al., 2007, ApJS, 173, 185
Hatano K., Branch D., Fisher A., Starrfield S., 1997, ApJ, 487, L45
Hays E., Cheung T., Ciprini S., 2013, The Astron. Telegram, 5302
Hoffmeister C., 1949, Veroff. Sternw. Sonnebrerg, 1, 295
Izzo L., Mason E., Vanzi L., Fernandez J. M., Espinoza N., Helminiak K., Della Valle M., 2013, The Astron. Telegram, 5639
Kolotilov E. A., Munari U., Popova A. A., Tatarnikov A. M., Shenavrin V. I., Yudin B. F., 1998, Astron. Lett., 24, 451
Kolotilov E. A., Shenavrin V. I., Shugarov S. Y., Yudin B. F., 2003, Astron. Rep., 47, 777
Liller W., Mayer B., 1987, PASP, 99, 606
Linford J. D. et al., 2015, ApJ, 805, 136
Max-Planck-Institut für extraterrestrische Physik, 2015, M31 (apparent) Optical Nova Catalogue. Available at: http://www.mpe.mpg.de/m31novae/opt/m31/index.php
Meinunger L., 1966, Mitt. Veranderl. Sterne, 3, 111
Mukai K., 2016, Koji's List of Recent Galactic Novae. Available at: http://asd.gsfc.nasa.gov/Koji.Mukai/novae/novae.html
Munari U., Margoni R., Stagni R., 1990, MNRAS, 242, 653
Munari U., Henden A., Dallaporta S., Cherini G., 2013, Inf. Bull. Var. Stars, 6080
Osborne J. P., Beardmore A., Page K., 2013, The Astron. Telegram, 4727
Özdönmez A., Güver T., Cabrera-Lavers A., Ak T., 2016, MNRAS, 461, 1177
Pietsch W., 2010, Astron. Nachr., 331, 187
Pietsch W. et al., 2007, A&A, 465, 375
Raj A., Banerjee D. P. K., Ashok N. M., 2013, MNRAS, 433, 2657
Ribeiro V. A. R. M., Munari U., Valisa P., 2013, ApJ, 768, 49
Savage B. D., Mathis J. S., 1979, ARA&A, 17, 73
Schlafly E. F., Finkbeiner D. P., 2011, ApJ, 737, 103
Seach J., 2015, Cent. Bur. Electron. Telegrams, 4080
Seach J. et al., 2013, Cent. Bur. Electron. Telegrams, 3732, 1
Shafter A. W., 1997, ApJ, 487, 226
Shafter A. W. et al., 2015, ApJS, 216, 34
Shara M. M., 1989, PASP, 101, 5
Shore S. N., De Gennaro Aquino I., Schwarz G. J., Augusteijn T., Cheung C. C., Walter F. M., Starrfield S., 2013, A&A, 553, A123
Shore S. N. et al., 2014, The Astron. Telegram, 6413
Simien F., Pellet A., Monnet G., Athanassoula E., Maucherat A., Courtes G., 1978, A&A, 67, 73
Wagner R. M. et al., 2012, The Astron. Telegram, 4157
Williams R., 2012, AJ, 144, 98
Yamaoka H., Itagaki K., 2009, Cent. Bur. Electron. Telegrams, 2050, 1

This paper has been typeset from a TEX/LATEX file prepared by the author.